PAPER

Check for updates

Cite this: *RSC Adv.*, 2020, **10**, 21318

Insight into the anti-aging mechanisms of natural phenolic antioxidants in natural rubber composites using a screening strategy based on molecular simulation†

Ling Lu,[a] Kaiqiang Luo,[a] Wei Yang,[b] Sidian Zhang,[a] Wencai Wang, [ID] [a] Haiyan Xu [ID] *[c] and Sizhu Wu [ID] *[a]

The failure of materials upon aging has led to the accumulation of waste and environmental pollution. Adding antioxidants (AOs) to the composites is one of the most effective ways to retard aging. However, traditional synthetic AOs are always detrimental to the environment and human health. The selection of antioxidants from streams by experiments will also definitely cost a lot of time and money. In addition, the complexity of thermo-oxidative aging factors along with the lack of quantitative tools significantly hampers its applications. So, building a screening strategy to quickly and easily find an appropriate and eco-friendly AO is imperative. In this study, we chose natural rubber (NR) as a matrix and provided a screening strategy based on diverse natural phenolic antioxidants to evaluate their ability in protecting NR composites. Thymol, α-tocopherol, and lipid-soluble epigallocatechin gallate (lsEGCG) were chosen from 18 natural phenolic antioxidants as potential alternative candidates. They were proved, indeed, to enhance the oxidative time in NR from experiments. Our results emphasized that thymol, α-tocopherol, and lsEGCG were promising alternatives for AOs in NR, and the *in vitro* toxicity test suggested that they are biocompatible. This study may develop a new strategy preference for screening the antioxidants by combining molecular simulation with the validation of experimental approaches, and therefore guide the AO molecular design with a more accurate theoretical prediction.

Introduction

In the last decade, the rubber production capacity has increased significantly with an average annual increase rate of 16.1%.[1] However, rubber materials are prone to oxidation under the condition of heat, oxygen, and other parameters. These conditions have an adverse effect on its performance, and are also severely detrimental to its service life.[2–5] To delay the thermo-oxidative aging, adding synthetic antioxidants have been effectively used in a rubber matrix.[6,7] Normally, antioxidants are viewed as effective additives, protecting materials against subsequent aging and opening opportunities as an inhibitor component of polymers, *e.g.*, plastic and rubber. Terminating the proxy radicals induced by heat has already been revealed to be a protective mechanism for the thermo-oxidative resistance

of polymers.[8] However, many traditional antioxidants such as the amine antioxidants N-1,3-dimethylbutyl-N′-phenyl-p-phenylenediamine (4020)[9] or N-cyclohexyl-N′-phenylbenzene-1,4-diamine (4010NA)[10] and the phenolic antioxidant butylated hydroxytoluene (BHT)[11] or butylated hydroxyanisole (BHA),[12] are toxic, which failed to pass the latest EU REACH environmental protection certification. Although synthetic AOs are protective additives, opening questions remain about the hazards of body contact and toxic pollution to the environment.[13–15] In contrast, natural AOs have advantages over traditional AOs, including their high efficiency and safe aspects, especially in drugs and food applications.

Many representative kinds of natural phenolic antioxidants are frequently used in medicines and food additives, which can be classified as flavonoids, vitamins and monophenols. However, the anti-oxidative stability of natural phenolic compounds in the polymer fields is seldom discussed.[16–18] Several research studies focused on the evaluation of the AO effectiveness. For example, α-tocopherol was revealed as a natural additive in polymer materials.[19,20] It was used as a radical scavenger in low density polyethylene, and was shown to be more efficient than the commercial antioxidants Irganox 1010 and 1076.[21] In addition, the results demonstrated that the

[a]State Key Laboratory of Organic–Inorganic composites, Beijing University of Chemical Technology, Beijing 100029, P. R. China. E-mail: wusz@mail.buct.edu.cn

[b]Global Energy Interconnection Research Institute, State Key Laboratory of Advanced Power Transmission Technology, Beijing 102211, P. R. China

[c]Institute of Basic Medical Sciences, Chinese Academy of Medical Sciences, Peking Union Medical College, Beijing 100005, P. R. China. E-mail: xuhy@pumc.edu.cn

† Electronic supplementary information (ESI) available. See DOI: 10.1039/d0ra03425h
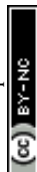
incorporation of phosphite-type secondary antioxidants with α-tocopherol remarkably enhanced the thermo-oxidative resistance due to a synergetic effect, and reduced the consumption rate of α-tocopherol.[22]

In fact, selecting effective alternatives from hundreds of natural AOs for polymer materials is tentatively in investigation.[23–25] Guitard *et al.* reported a comparative assay that followed the investigation of the antioxidant activity of phenols. It was shown that myricetin and rosemary acids were represented as challenging alternatives for synthetic antioxidants.[20] Furthermore, several modified ester derivatives of rosmarinic acids were assessed using the 2,2-diphenyl-1-picrylhydrazyl (DPPH) test, and the measurement of oxidative induction time and accelerated thermo-aging tests.[25] The effect of dihydromyricetin on the dispersion situation of linear low density polyethylene was also evaluated by the changing color of the compounds. It was shown that dihydromyricetin retained high stability against migration.[26] Herein, Öncel *et al.* investigated the antioxidant ability of Henna for an efficient and conventional sulfur vulcanization system in NR compounds by comparing it with that of TMQ.[15] In addition, the oxidation resistance of ethylene propylene diene monomer (EPDM) was demonstrated to be enhanced by naringenin and caffeic acid. In addition, the EPDM composites with a higher concentration of antioxidants had a much higher oxidative induction time (OIT), even in the irradiated environment.[21] Consequently, the application of natural AOs in polymers demonstrated that the antioxidants' activity and migration ability were important factors for improving the long-term protective efficiency.[26] However, most research studies of these AOs were qualitatively investigated through experiments. The quantification of the antioxidation factors of natural AOs from the perspective of the microscopic molecular level is still limited.

Molecular simulation is a cost-effective method to quantitatively analyze the relationship between microstructure and performance.[3,27] For example, the quantum mechanics (QM) method has been used to calculate the free energy of dissociation from the point of view of the chemical reaction. Some physical parameters, including solubility parameter (δ), mean square displacement (MSD), diffusion coefficient (D) and solution coefficient (S), can be computed by the molecular dynamics (MD) method, which could provide quantitative results and predict the physical parameters of the materials.[28,29] Yu *et al.* clearly predicted the antioxidant activity by calculating the dissociation energy quantitatively based on the DFT method, and hence explored the underlying mechanism of antioxidants.[30] In addition, a new type of antioxidant-modified silica was reported to improve the dispersion state in solution-polymerized styrene butadiene by MD calculation.[31,32] Therefore, this was the motivation to derive a simulation method for computing the chemical and physical anti-oxidation parameters, which are usually difficult to obtain from experiments.[6,10,32] It might be an effective attempt to select the valid natural AOs in a wide variety of ranges for NR composites.

In this work, we aim to build a predictive strategy of screening the effective phenolic antioxidants from streams of natural antioxidants by means of molecular simulation. The mechanisms of high-efficiency and the thermo-oxidative of the AO/NR systems were investigated through the combination of simulation and experimental methods, and the toxicity test was also evaluated.

Molecular simulation processes

Molecular simulations, including quantum mechanics (QM) simulation, molecular dynamics (MD) simulation, and Monte Carlo (MC) simulation,[3,29,33] which were performed using the Materials Studio (MS) software (Accelrys Software Inc.), provided a tool to screen for effective phenolic antioxidants. The procedure is described in the following sections.

Quantum mechanics (QM) simulation

The free energy of dissociation (ΔG) for active hydrogen in AOs and NR, *i.e.*, the free energies of O–H bond dissociation in AOs and the C–H bond dissociations at different positions in NR, were computed by QM methods. The results of the dissociation energy were given and discussed according to the hydrogen atom transfer (HAT) mechanism of the antioxidant.[29]

The QM simulations were based on density functional theory (DFT) and were performed on the Dmol³ module. To calculate the thermodynamic properties as a function of temperature, a frequency analysis was used for the full geometry optimization. The detailed parameters were set up as follows: the exchange–correlation potential was determined by the generalized gradient approximation (GGA) in the form of the Perdew–Burke–Ernzerhof (PBE) function. All electrons with no special treatment and the atomic orbital basic set Triple Numerical plus Polarization (TNP) were chosen to calculate the external potential.[34] For the free radical, the multiplicity was set as a doublet in the spin unrestricted condition. To obtain fully optimized structures, the self-consistent field (SCF) procedure with a convergence threshold of 10^{-6} au and fine criteria for convergence qualities were employed in a Dmol³ Geometry Optimization task.

Molecular dynamics (MD) simulation

The physical parameters (*e.g.*, diffusion coefficient (D), solution coefficient (S), solubility parameter (δ), mean square displacement (MSD)) were calculated in the molecular dynamics (MD) simulation to explore the process of oxygen entering the rubber matrix, and the compatibility and migration ability of the antioxidants. The amorphous cell and Forcite modules in MS with the condensed-phase optimized molecular potentials (COMPASS) force field were applied in the whole simulation process. The amorphous cell model of the neat NR, AO, AO/NR and AO/O_2/NR systems were constructed as shown in Fig. 1. Taking the AO/NR system as an example, four NR molecular chains with 200 repeat units were put in an amorphous cell with 30 antioxidant molecules, and then the full geometry optimization was employed. This cell experienced a range of annealing and dynamics processes to achieve the complete equilibrium. The amorphous cell was minimized by 200 000 steps of energy minimization with the smart minimizer method.[29] In addition,
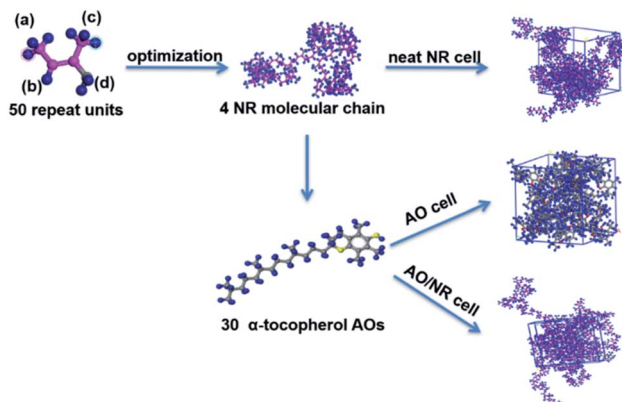
Fig. 1 Construction processes of the neat NR, AO (take α-tocopherol as an example) and AO/NR amorphous cells (the magenta, blue and yellow represent C, H and O atoms, respectively).

Fig. 2 Thermo-oxidative aging reaction of rubber (RH) in the presence of antioxidant (AH).

the minimized cell was annealed from 298 to 500 K for 100 annealing cycles with the heating ramps per circle under 200 ps of the NVE ensemble (constant number of atoms, constant volume and constant energy). After that, the annealed cell was further relaxed through 200 ps of the NVT (constant number of atoms, constant volume and constant temperature) ensemble dynamic simulations. Finally, the cell reached equilibrium after at least 1000 ps under NPT ensemble (constant number of atoms, constant pressure, and constant temperature). Above all sets of MD simulations, Andersen thermoset and Berendsen barostat were used to control the temperature and pressure, respectively.[35–37] Similarly, the neat NR, AO and AO/O_2/NR systems were also constructed and ran in the programs.

Theoretical results and discussion

Antioxidants screening process

The aim of this work was to screen high efficiency antioxidants based on a diverse set of natural phenolic antioxidants, and to explore the protective mechanisms. From the available literature on the characteristics of the antioxidant and the reactivity of NR in thermo-oxidative aging conditions,[15] the chemical and physical thermo-oxidative aging factors could be determined comprehensively. In addition, it was possible to analyze the relevant parameters, including the free energy of dissociation (ΔG), solubility parameter (δ), mean square displacement (MSD), diffusion coefficient (D), solution coefficient (S), among others. These parameters with a specific meaningful definition of antioxidants may predict the trend of the anti-aging effect of antioxidants, and were calculated quantitatively as described in the following sections.

The free energy of dissociation. As shown in Fig. 2, the bonds of rubber macromolecules are easily broken due to a large number of isolated double bonds, leading to the abstraction of active α-hydrogen under thermal-oxidative conditions,[2] thus producing alkyl radicals R·, peroxyl radicals ROO· and other free radicals. The AH antioxidants can capture free radicals, subsequently inhibiting the oxidation reaction and delaying the thermo-oxidative aging.[9,17] Therefore, the dissociation of an
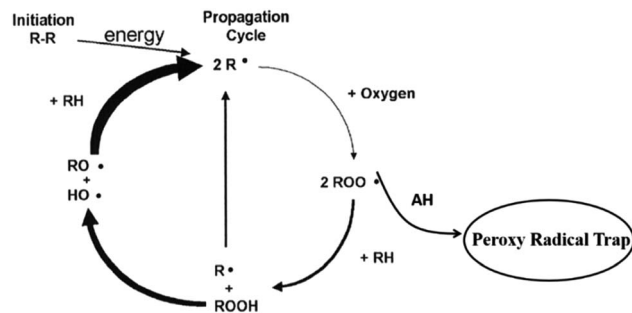
active hydrogen in antioxidants plays an extremely important role in the chemical aging protection. The free energies of O–H bond dissociation in phenolic antioxidants and α-hydrogen bond dissociation in NR can be calculated and compared with each other to quantitatively analyze the chemical protection efficiencies.[20] In this study, the free energies of the O–H bond dissociation of 18 natural phenolic antioxidants were calculated, and the corresponding results are listed in Table S1 (ESI†). The molecular structures of these natural phenolic antioxidants are shown in Fig. 4, of which dihydromyricetin (no. 1 in Fig. 4), quercetin (2), silymarin (3), curcumin (4), demethoxycurcumin (5) and bis-demethoxycurcumin (6) were selected as derivatives of the flavonoids. α-Tocopherol (7), β-tocopherol (8), γ-tocopherol (9), δ-tocopherol (10), and vitamin C (11) were considered for the vitamins class. Resveratrol (12), rosmarinic acid (13), lipid-soluble epigallocatechin gallate (lsEGCG) (14), astaxanthin (15) were the polyphenols types. Other antioxidants represented the monophenols, including lawsone (16), carvacrol (17) and thymol (18). It is known from the literature that as the free energies of the O–H bond dissociation decreased, the efficiencies of the natural phenolic antioxidants to capture free radicals became stronger, which is due
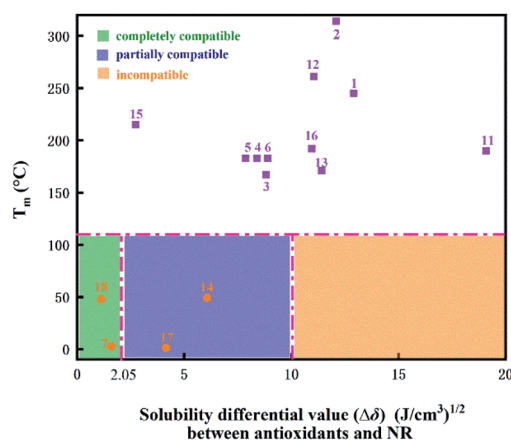

Fig. 3 The map shows 18 natural phenolic antioxidants with melting point T_m and the solubility differential value ($\Delta\delta$) between antioxidants and NR. The orange dots (no. 7, 14, 17, 18 samples) may be potential candidates according to $\Delta\delta$ and T_m values.
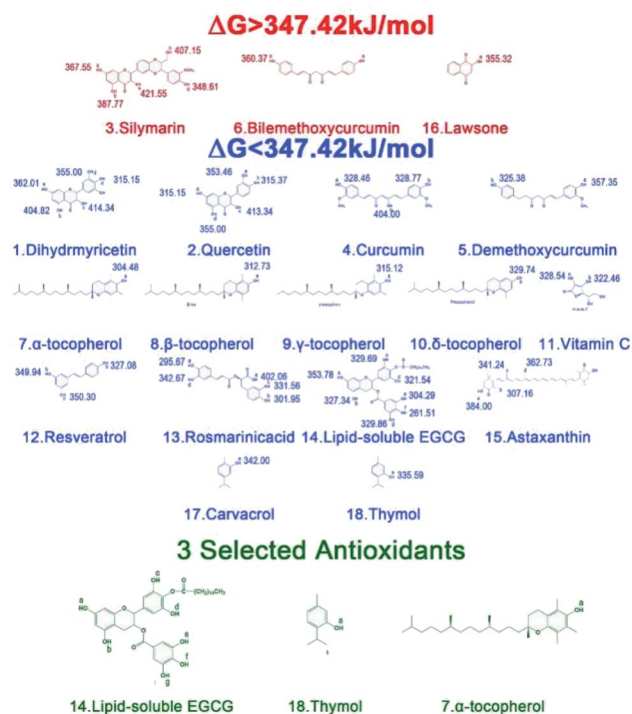
Fig. 4 Screening process of natural phenolic antioxidants and the ΔG (kJ mol^{-1}) of ArO−H bonds at different position are indicated in the structures.

Fig. 5 MSD curves of three selected antioxidants (thymol, α-tocopherol and lsEGCG) in NR matrix at (a) 298 K and (b) 373 K.

to the electron donating effect.[38] For example, the existence of alkyl radicals near the –OH group could lead to a decrease in the free energies of dissociation. The free energies of bis-demethoxycurcumin (6), demethoxycurcumin (5) and curcumin (4) were 360.37, 357.35 and 328.46 kJ mol^{-1}, respectively, and are indicated in Table S1.†

Meanwhile, the free energies of the C–H bond dissociation in NR were calculated (as shown in Table S2†) with the lowest value of 347.42 kJ mol^{-1} at the position (a). When the free energy of dissociation of the O–H bond in an antioxidant is lower than that of the (a) position (here is 347.42 kJ mol^{-1}), the antioxidant can preferentially dissociate first and effectively inhibit the oxidation of NR.[6] According to the above analysis, except for silymarin (3), bilemethoxycurcumin (6) and lawsone (16) (red colors in Fig. 4), it is theoretically predicted that the other 15 natural phenolic antioxidants (blue colors in Fig. 4) could play a chemical protective role in the NR matrix.

Solubility parameters. The solubility parameters of antioxidants (the free energy of dissociation is less than 347.42 kJ mol^{-1}, which is indicated with blue colors in Fig. 4) were calculated, and the solubility differential value ($\Delta\delta$) between the antioxidants and NR is shown in Fig. 3. The solubility parameters could be used to evaluate the compatibility of the mixing materials.[39] According to the semi-empirical approach, $\Delta\delta = |\delta_{antioxidant} - \delta_{NR}|$, if $\Delta\delta$ is less than 2.05 (J cm^{-3})$^{1/2}$, then they are completely compatible. When $\Delta\delta$ is between 2.05 (J cm^{-3})$^{1/2}$ and 10.02 (J cm^{-3})$^{1/2}$, they are partially compatible.[6] The simulated solubility parameter of NR was 16.30 (J cm^{-3})$^{1/2}$. Therefore, two natural phenolic antioxidants
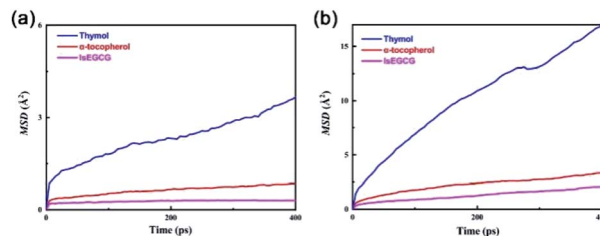
could be further screened, including α-tocopherol 7 (17.89 (J cm^{-3})$^{1/2}$) and thymol 18 (17.43 (J cm^{-3})$^{1/2}$). At the same time, the antioxidants that met the demands of the rubber processing temperature range from 80 °C to 110 °C were obtained by determining the suitable melting point (T_m) for good dispersion in the rubber matrix. They were α-tocopherol 7 (2.5–3.5 °C), lsEGCG 14 (49–62 °C), carvacrol 17 (1 °C) and thymol 18 (48–52 °C) (orange dots in Fig. 3). Although the δ value of lsEGCG was 22.38 (J cm^{-3})$^{1/2}$, the XRD analysis showed that the crystallization peak position of lsEGCG (no. 14) in the NR matrix had decreased in comparison to that of the lsEGCG powder, which proved that the crystal was destructed in the manufacturing process, and could be compatible and stable in the rubber matrix (shown in Fig. S2†). In addition, the differential $\Delta\delta$ between thymol (18), α-tocopherol (7) and NR was 1.13 and 1.59 (J cm^{-3})$^{1/2}$, respectively, indicating that they might be better dispersed in the rubber matrix and had excellent compatibility with the NR compounds. Therefore, 3 kinds of antioxidants, which are lsEGCG (14), thymol (18) and α-tocopherol (7), were finally selected for the NR composites, as shown in Fig. 4 with green colors.

Mean square displacement (MSD). The migration trajectory of the antioxidant molecules was analyzed in the rubber matrix, which is related to the physical process of the antioxidants entering the rubber matrix. The mean square displacement (MSD) values of the antioxidants were obtained from the following equation:[40]

$$\text{MSD} = \langle |r_i(0) - r_i(t)|^2 \rangle \tag{1}$$

where $r_i(t)$ and $r_i(0)$ represent the positions of atom i at time t and initial time 0, respectively. $|r_i(0) - r_i(t)|$ is the displacement of atoms i in time t. Finally, the bracket means that the average of the square of the displacement is taken for all selected atoms.

The MSD curves of those three selected antioxidants in the NR matrix at 298 K and 373 K are shown in Fig. 5. The value of the MSD of thymol was higher than that of α-tocopherol and lsEGCG at both 298 K and 373 K, where the MSD value of lsEGCG was the minimum one. In addition, the MSD value was higher at the high temperature, agreeing with the fact that the antioxidant molecules migrated faster at the high temperature. With the minimum MSD value, it was demonstrated that the lsEGCG retained high stability against migration, and was then followed by α-tocopherol and thymol.

Oxygen permeability. Based on the thermo-oxidative aging mechanisms discussed in the previous section, it is known that

Table 1 The D, S and P values for O_2 in the NR and AOs/NR systems

System	D (10^{-6} cm^2 s^{-1})	S (10^{-3} cm^3 (STP) cm^{-3} kPa^{-1})	P (10^{-9} cm^2 s^{-1} kPa^{-1})
NR	3.7 ± 0.8	1.6 ± 0.3	5.9
Thymol/NR	1.8 ± 0.5	1.7 ± 0.8	3.1
α-Tocopherol/NR	1.4 ± 0.5	1.6 ± 0.2	2.2
lsEGCG/NR	0.8 ± 0.2	1.9 ± 0.6	1.5

oxygen was easier to react with alkyl radicals to produce peroxyl radicals, which further triggered a series of aging reactions. During this process, the O_2 permeability is the key physical factor for the antioxidants to protect the materials from aging.[29] The formula based on the classical dissolve-diffusion model is as follows:

$$P = D \times S \qquad (2)$$

where D is the diffusion coefficient and S is the solution coefficient. The diffusion coefficient of the molecular chains can be calculated by the following Einstein equation:[33]

$$D = \frac{1}{6N} \lim_{t \to \infty} \frac{\mathrm{d}}{\mathrm{d}t} \sum_{i=1}^{N} \left\langle [r_i(t) - r_i(0)]^2 \right\rangle \qquad (3)$$

where N represents the total number of particles in the system.

S is obtained by the dual-mode sorption model.[33] The model is described as:

$$C = K_D p + \frac{C_H bp}{1 + bp} \qquad (4)$$

Then, S can be further deduced as:

$$S = \lim_{p \to 0} \left(\frac{C}{p} \right) = K_D + C_H b \qquad (5)$$

The calculated D, S and P values for O_2 in the NR and AOs/NR systems are listed in Table 1. It could be seen that the P value of lsEGCG was the minimum, followed by α-tocopherol and thymol. In addition, the permeability coefficient P of AO/NR was obviously lower than that of the neat NR system, which revealed that the antioxidants indeed had an effect on the oxygen barrier ability of the NR composites. Combined with the previous result of the MSD value shown in Fig. 5, it can be speculated that the three selected antioxidants could certainly play a role in anti-oxidative stability. In addition, the anti-aging efficiency may be predicted following the order as lsEGCG > α-tocopherol > thymol. Therefore, the next sections describe the experimental verification according to this theoretical inference.

Experimental materials and characterization methods

Materials

Natural rubber (NR) was supplied by Tianjin Changli Rubber Trade Co., Ltd. The antioxidants were thymol (Acros, China, 99%), α-tocopherol (Shanghai Jiuding Chemical Co., Ltd.,

China, 96%) and lipid-soluble epigallocatechin gallate (lsEGCG, Hangzhou Puremedie Biological Technology Co., LTD., China, 90%). Carbon black N330 (CB N330) was purchased from Qingdao Degussa Chemical Co., Ltd. Other rubber auxiliaries, including zinc oxide (ZnO, CP), stearic acid (SA, CP), sulfur (S), and N-cyclohexyl-2-benzothiazole sulphonamide (CZ, CP), were industrial grade products. All of the abovementioned materials were used without further refinement.

Preparation of NR composites

Two-roll mill was used for preparing the NR compound following the formulations which is shown in Table 2. The curing characteristics (e.g., minimum torque M_L, maximum torque M_H, scorch time t_{10}, and optimum cure time t_{90}) for NR samples were tested on a curometer without rotator at 143 °C, and then the NR composites were obtained by vulcanization on a flat vulcanizing machine with the pressure of 15 MPa at 143 °C for t_{90} + 2 min. Finally, the NR composites with 2 mm in thickness were trimmed into the dumb-bell shaped specimens for aging and mechanical tests according to GB/T3512-2001 standard.

Characterization methods

DPPH (2,2-diphenyl-1-picrylhydrazyl) test. The free radical scavenging activity of the antioxidants were determined using a DPPH (2,2-diphenyl-1-picrylhydrazyl) method previously described in the literature.[20] The DPPH solution (100 μmol L^{-1}, 200 μL) was added to the antioxidant solution (50 μmol L^{-1}, 50 μL) in a 96-well plate. The mixed solutions were kept for 30 min at room temperature without light, and were measured in the DPPH absorbance at 520 nm with a microplate reader (BioTek, USA). The mixed samples were compared against a blank or control [containing distilled water (50 μL)/ethanol (200 μL) or distilled water (50 μL)/DPPH regent (200 μL), but without

Table 2 The formula of the NR composites[a]

Ingredients (phr)	Sample symbols[b]					
	1	2	3	4	5	6
NR	100	100	100	100	100	100
Antioxidants	—	1.36	3.91	1.05	2.11	6.32

[a] Other rubber additives: ZnO, 5 phr (parts per hundreds of rubber); SA, 2 phr; CZ, 1.5 phr; CB N330 50 phr; S, 2 phr. [b] Sample symbols 1, 2, 3 represent NR, thymol/NR, α-tocopherol/NR, respectively. Sample symbols 4, 5, 6 represent the lsEGCG/NR with different contents of 1.05, 2.11 and 6.32 phr, respectively.

antioxidants]. The percentage of the DPPH scavenging activity was calculated as shown in eqn (6),[41] of which A_c, A_s, A_b are represented as the absorbance of the control, sample and blank, respectively.

Percentage of DPPH scavenging activity (%) =
$$(A_c - A_s)/(A_c - A_b) \times 100\% \quad (6)$$

Accelerated thermo-oxidative aging experiments. The dumbbell shaped NR composites were subjected to accelerated thermo-oxidative aging for different aging times (0, 1, 3 and 5 days) at 100 °C in an air-circulating heating cabinet oven (GT-7017-E, Gotech Testing Machines Co., Ltd., China).

Mechanical test. The dumb-bell shaped samples were tested before and after aging on an electrical tensile instrument (CMT4104, Shenzhen SANS Testing Machine Co., Ltd., China) with a tensile speed of 500 mm min^{-1}. The mechanical properties (tensile strength σ, elongation at break ε_{break}) of the NR composites were calculated, and the average values of five parallel samples were reported with standard deviation.

Oxidative stability observation. The oxidation induction time (OIT) was measured using differential scanning calorimetry (DSC) (Mettler Toledo Corporation, TA Instruments, Switzerland).[42] The samples ($\sim$5 mg) were placed in an uncovered aluminum pan and heated from 25 °C to 180 °C at the rate of 30 K min^{-1} under nitrogen flowing at 50 mL min^{-1}. After equilibrating for 5 min, the purge was switched to pure oxygen flow. The OIT was determined by the exothermal oxidation peak point of the curve. The oxidative onset temperature (OOT) was determined by heating from 25 °C to 300 °C at a rate of 10 K min^{-1} under an oxygen flow of 50 mL min^{-1}.

Fourier transform infrared spectroscopy (FT-IR). The chemical structures for the NR compounds were recorded on an FT-IR spectrometer (Bruker Tensor 27, Germany) with the Attenuated Total Reflectance (ATR) mode. The scanning wavenumber was in the range of 400 to 4000 cm^{-1} with a resolution of 4 cm^{-1}.

X-ray diffraction (XRD). The XRD measurements were carried out using a Shimadzu XRD-6000 powder X-ray diffraction unit with Cu Kα at 30 mA and 30 kV, in the 2θ range of 5° to 90°.

Biocompatibility evaluation. The cytotoxicity test of the natural phenolic antioxidants was analyzed via a cell MTT assay in the MC3T3 cell line. The cells were cultured in MEM Alpha Modification medium (MEM, HyClone, USA) with 10% fetal bovine serum and 2% penicillin–streptomycin solution (HyClone, USA) in an incubator under a humidified atmosphere of 5% CO$_2$ at 37 °C. Then, the unattached cells were removed and fresh culture medium was replaced every other day until reaching almost 90% confluence for sub-culturing. After that, cells were seeded on the cross sections parallel to the axis direction of the sterilized samples in a 96-well plate. After incubating for 1, 2 and 3 days, the absorbance at 630 nm was measured using a microplate reader (BioTek, USA).[43]

Experimental results and discussions

Antioxidant activity

The DPPH test is typically used to determine the free radical scavenging activity of the antioxidants due to the hydrogen atom abstraction by the DPPH radical.[20] The mechanism is shown in the following equation:
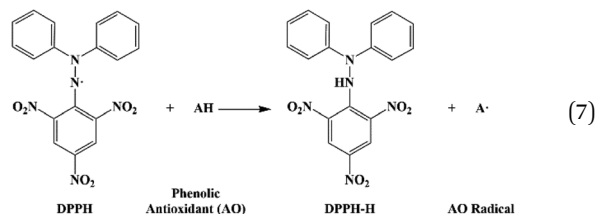
In fact, it is typical to abstract a hydrogen atom from the antioxidants to react with the radical, which competes with the chemical process of the reaction between the radical and the rubber chains. The antioxidant activity of monophenol could be obtained and the antioxidant activity of α-tocopherol is slightly higher than thymol, which is shown in Fig. 6. The dosage of the antioxidants in the DPPH test was kept at the same molar ratio as that in the simulation model. The antioxidant activity of monophenol with the DPPH test was consistent with the previously calculated results of the free energy of dissociation, which proved the prediction of the theoretical results. Here, the lsEGCG was found to have the highest antioxidant activity owing to its six effective hydroxyl groups.

Curing characteristic of NR composites

Fig. 7 shows the curing curve of the NR composites at 143 °C, and the analyzed curing parameters are listed in Table 3. It should be noted that the dosage of the antioxidants was kept at the same molar ratio as that in the simulation model. For α-tocopherol, it is an oily liquid small molecule. The presence of α-tocopherol in NR has an influence on vulcanization due to the plasticization of α-tocopherol.

The torque difference (ΔM) between the maximum torque (M_H) and the minimum torque (M_L) is proportional to the cross-linking degree, which is an indirect measure of the modulus
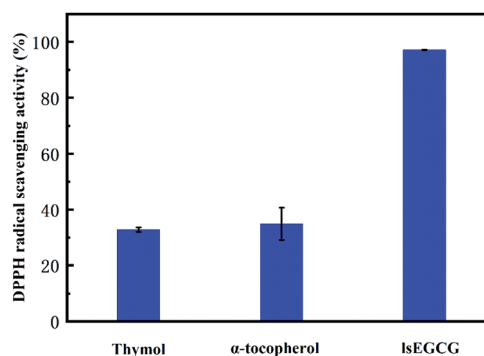

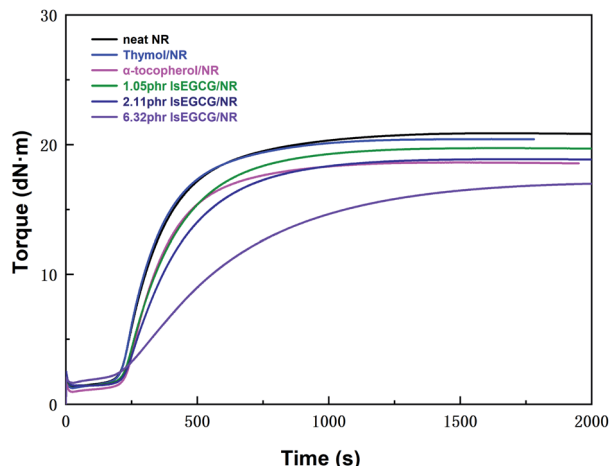**Fig. 6** DPPH radical scavenging activity values of three antioxidants.

Fig. 7 Curing curves of the NR composites at 143 °C.

Table 3 Curing parameters of the NR composites

Samples	t_{10} (s)	t_{90} (s)	M_H (dN m)	M_L (dN m)	ΔM (dN m)
NR	248	688	20.49	1.27	19.22
Thymol/NR	249	604	20.04	1.20	18.84
α-Tocopherol/NR	241	634	18.27	0.91	17.36
1.05 phr lsEGCG/NR	278	703	19.36	1.38	17.98
2.11 phr lsEGCG/NR	250	739	18.52	1.39	17.13
6.32 phr lsEGCG/NR	288	1188	16.71	1.60	15.11

and cross-linking density. As seen in Table 3, the ΔM of α-tocopherol was also reduced to 17.36 dN m compared with neat NR (19.22 dN m). However, the NR composites with lsEGCG (6.32 phr) had a lower ΔM value (15.11 dN m) than α-tocopherol/NR. This occurred not only as a result of the plasticization of the free antioxidant lsEGCG, but also due to the phenolic antioxidants delaying vulcanization and affecting the cross-link density.[44] thus, these events led to the tensile strength being below the others. As we know, the excessive addition of antioxidants in practical application, especially phenolic types, could also delay vulcanization and affect the cross-link density and mechanical properties.[15] Compared with lsEGCG with 6.32 phr, the curing time (t_{90}) of the other AO/NR composites and neat NR systems were relatively close. lsEGCG with 1.05 phr was used in the formula to ensure the consistency of the molar ratio of the antioxidants, and lsEGCG with 2.11 phr was used as the usual dosage in the processing application. In this way, it not only reduced the consumption of the additives, but it also satisfied the requirements of the processing conditions.

Thermo-oxidative of NR composites

Mechanical performances of NR composites during aging process. The mechanical performances are an important aspect of evaluating the thermo-oxidative aging processes. The comparison columns of the tensile strength and elongation at the break of the NR composites before and after aging are
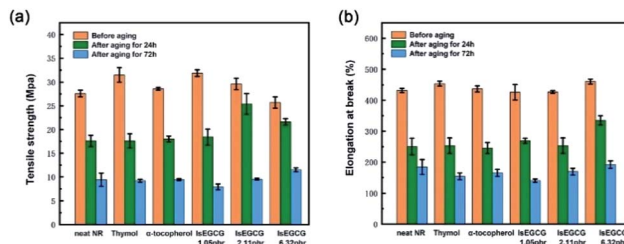

Fig. 8 (a) Tensile strength and (b) elongation at the break of NR composites before and after aging.

shown in Fig. 8. The NR composites with AOs showed a higher tensile strength than the neat NR composites before aging ($p < 0.05$). There was no significant change in the tensile strength of the AO/NR composites after aging for 24 h and 72 h, which is comparable to the neat NR after aging ($p > 0.05$). In contrast, the tensile strength of lsEGCG with 2.11 phr and 6.32 phr was 30.7% and 22.3% higher than that of the neat NR after aging for 24 h, suggesting that lsEGCG with 2.11 phr and 6.32 phr had a good short-term thermo-oxidative anti-aging effect. The tensile strength of lsEGCG with 6.32 phr decreased slightly in comparison to the 2.11 phr lsEGCG. This may be due to the excessive lsEGCG addition affecting the vulcanizates.[31] In addition, the elongation at the break of AOs/NR composites was comparable to that of the neat NR (shown in Fig. 8(b), $p > 0.05$), showing that the addition of the antioxidants had little influence on the elongation at break. In contrast, the NR composites with lsEGCG (6.32 phr) has a higher elongation at break ($p < 0.05$) due to the plasticization complex interaction between the plasticization and the vulcanization interference. Therefore, adding natural phenolic antioxidants have no adverse significance on the mechanical properties, even slightly improved, which is consistent with the conclusions drawn from the above curing characteristic of the NR composites in Fig. 7.

Oxidation stability of NR composites. The oxidation stability is an important indicator for evaluating the service life of materials.[20] It can be characterized by oxidation induction time (OIT) and oxidation onset temperature (OOT) by the thermal analysis experiments.[45] Both OIT and OOT assessments were performed on the crude masterbatch. Fig. 9 shows the OIT of the neat NR and AO/NR compounds at 180 °C. The OIT of neat NR was 19.4 min in the absence of AOs, and those of thymol and α-tocopherol were 21.2 min and 20.9 min, respectively. The OIT was dramatically prolonged with the increase of lsEGCG. The OIT of lsEGCG with 1.05 phr and 2.11 phr were 112% and 228% higher than that of neat NR, respectively. In addition, the oxidation exothermic peak still did not appear after adding lsEGCG with 6.32 phr for 70 min. In order to further evaluate the oxidation stability of natural phenolic AOs, the OOT of neat NR and AO/NR compounds were determined and are shown in Fig. 10. The OOT of NR compounds with the introduction of antioxidants was 29.67% higher than that of neat NR. The 6.32 phr lsEGCG/NR samples with an OOT value of 282.3 °C showed the best antioxidant stability, followed by α-tocopherol and thymol. These results were consistent with that of the simulated anti-aging effect of the antioxidant. Likewise, the
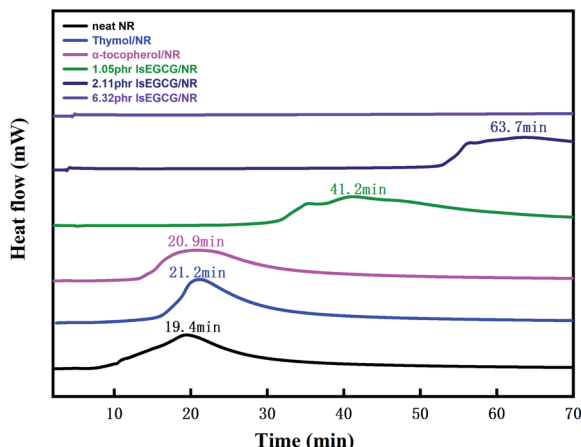
Fig. 9 Oxidation induction time (OIT) assessment of antioxidants/NR at 180 °C.

OOT was also elevated greatly with the increase of the dosage of lsEGCG, indicating that it exactly corresponded to the previous trend of OIT.

Microstructure analysis of NR composites

NR composites produce different oxidation products (*e.g.*, esters, lactones) during the thermal-oxidative aging process.[2] The addition of natural phenolic antioxidants could delay the aging of the NR composites based on the above results of the mechanical properties and oxidation stability tests. The content change of the carbonyl group of different AO/NR compounds before and after thermo-oxidative aging for 1, 3 and 5 days were observed at 100 °C, as shown in Fig. 11. The carbonyl group content increased with the formation of oxidation products as the aging time increased. In addition, the increase rate of the carbonyl group in the AO/NR compounds decreased significantly in comparison with the blank sample. It was shown that the symmetrical stretching vibration of CH_2 at 2848 cm^{-1} was not affected by thermal oxidation aging.[46] Therefore, the carbonyl increase rate, *i.e.*, the ratio of C=O (1736 cm^{-1}) to CH_2 (2848 cm^{-1}) ($A_{(C=O)}/A_{(CH_2)}$), could quantitatively be revealed as

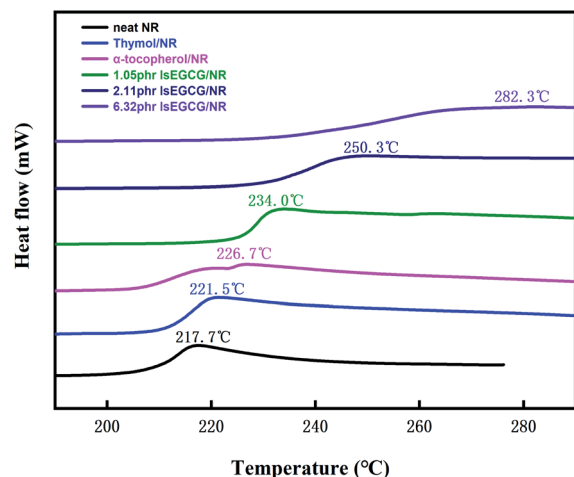**Fig. 10** OOT assessment of the neat NR and antioxidants/NR.

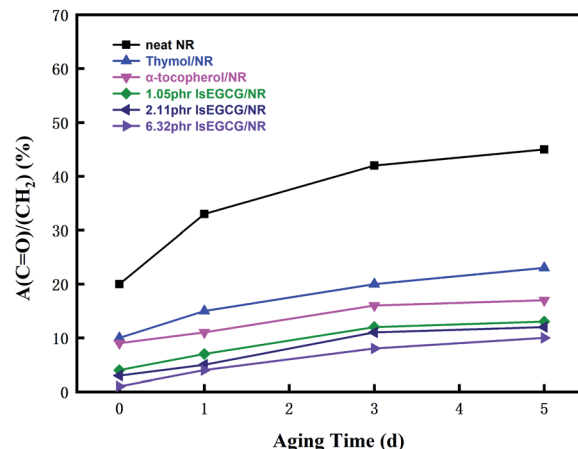**Fig. 11** The ratio of $A_{(C=O)}/A_{(CH_2)}$ with different antioxidants/NR composites after thermo-oxidative aging times for 1, 3 and 5 days at 100 °C.

the thermal-oxidative aging degree of the NR composites. It was found that the natural phenolic antioxidants could effectively delay the formation of the oxidation products with the lower $A_{(C=O)}/A_{(CH_2)}$ values, and play a protective role in the NR composites. When the dosage of lsEGCG increased from 1.05 phr to 6.32 phr, the carbonyl increase rate decreased correspondingly. Moreover, the sequence of the carbonyl increase rate was lsEGCG < α-tocopherol < thymol, just as evidenced by the previous thermo-oxidative performances.

In vitro cytotoxicity test

In order to detect whether the introduction of natural phenolic antioxidants was non-toxic and biocompatible in NR composites, MC3T3 cells were qualitatively used to test the cytotoxicity of antioxidants based on the relative growth rate (RGR) of cells. When the RGR of cells was over 90%, the measured materials
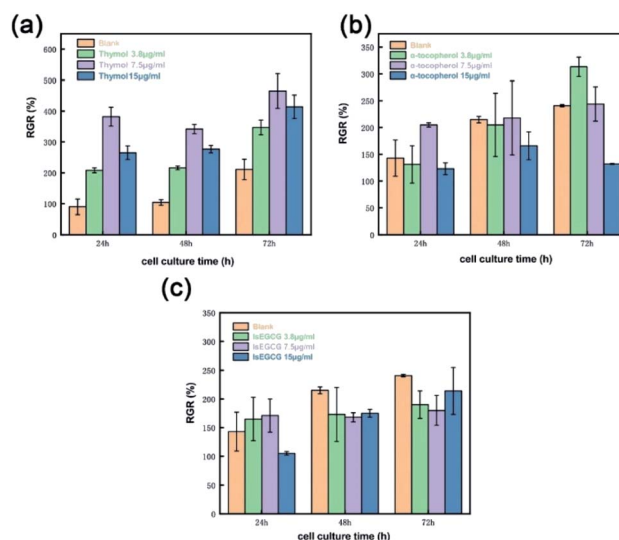

Fig. 12 RGR (%) of the MC3T3 cells cultured in (a) thymol, (b) α-tocopherol and (c) lsEGCG antioxidants solution with different doses.

were considered to meet the requirements of the non-toxic material standard, as mentioned in the literature.[43,47] According to the optical density (OD) value measured by a microplate reader at 630 nm, the RGR of the cells could be calculated from the following formula:[43]

$$RGR = \frac{OD_{test} - OD_0}{OD_{control} - OD_0} \times 100\% \quad (8)$$

where $OD_{control}$, OD_{test} and OD_0 are the optical density values of control, sample and blank, respectively.

From Fig. 12, the RGR value of the MC3T3 cells was more than 100% at different times and concentrations for all samples. Although the RGR of the samples decreased slightly at 15 μg mL^{-1} concentration, it had no adverse effect on the cell growth, indicating that the simulation-selected natural phenolic antioxidants, i.e., thymol, α-tocopherol and modified lipid-soluble EGCG, were all non-toxic and biocompatible.

Conclusions

In this work, a molecular simulation method preference for screening the environmentally friendly natural antioxidants with the twin goals, i.e., non-toxicity and high anti-aging efficiency, was presented. First, 18 kinds of natural phenolic antioxidant dissociation energies were calculated by the quantum mechanics (QM) method. Then, the effect of the selected natural AOs on the NR composites was analyzed using the molecular dynamics (MD) method to explore the solubility difference, mobility of the AOs and the permeability of O$_2$ in the NR matrix. According to the quantification of the anti-oxidation factors of natural AOs from the perspective of the microscopic molecular level, thymol, α-tocopherol and lsEGCG were selected to demonstrate 3 kinds of AOs for NR composites.

Experimentally, the 2,2-diphenyl-1-picrylhydrazyl (DPPH) test proved the effectiveness of the predicted outcomes. This was reinforced by their performance in terms of curing, mechanical and thermo-oxidative resistance of the NR composites from the macrostructure and microstate aspects. Additionally, combined with the in vitro cytotoxicity test, the modified natural antioxidant lsEGCG showed the best properties and biocompatible performance.

This work not only brings insights into the underlying protective mechanisms for NR, but also delivers an effective strategy for screening the antioxidants. It may also show a potential application in antioxidant molecular design.

Conflicts of interest

There are no conflicts to declare.

Acknowledgements

Notes and references

1 M. Sol-Sánchez, F. Moreno-Navarro, L. Saiz and M. C. Rubio-Gámez, *J. Cleaner Prod.*, 2020, **244**, 118570.

2 M. Komethi, N. Othman, H. Ismail and S. Sasidharan, *J. Appl. Polym. Sci.*, 2012, **124**, 1490–1500.

3 C. Li and A. Strachan, *J. Polym. Sci., Part B: Polym. Phys.*, 2015, **53**, 103–122.

4 L. Bokobza, *Nanomaterials*, 2019, **9**, 12.

5 L. P. Lim, J. C. Juan, N. M. Huang, L. K. Goh, F. P. Leng and Y. Y. Loh, *Mater. Sci. Eng., B*, 2019, **246**, 112–119.

6 W. Zheng, Y. Wu, W. Yang, Z. Zhang, L. Zhang and S. Wu, *J. Phys. Chem. B*, 2017, **121**, 1413–1425.

7 J. Yang, Y. Huang, Y. Lv, S. Li, Q. Yang and G. Li, *Carbon*, 2015, **89**, 340–349.

8 E. Rojo, M. S. Peresin, W. W. Sampson, I. C. Hoeger, J. Vartiainen, J. Laine and O. J. Rojas, *Green Chem.*, 2015, **17**, 1853–1866.

9 M. De Lucia, L. Panzella, A. Pezzella, A. Napolitano and M. d'Ischia, *Tetrahedron*, 2006, **62**, 1273–1278.

10 N. Ning, Q. Ma, Y. Zhang, L. Zhang, H. Wu and M. Tian, *Polym. Degrad. Stab.*, 2014, **102**, 1–8.

11 W. A. Yehye, N. A. Rahman, A. Ariffin, S. B. Abd Hamid, A. A. Alhadi, F. A. Kadir and M. Yaeghoobi, *Eur. J. Med. Chem.*, 2015, **101**, 295–312.

12 G. M. Williams, M. J. Iatropoulos and J. Whysner, *Food Chem. Toxicol.*, 1999, **37**, 1027–1038.

13 S. Wu, P. Weng, Z. Tang and B. Guo, *ACS Sustainable Chem. Eng.*, 2015, **4**, 247–254.

14 S. Wu, M. Qiu, B. Guo, L. Zhang and Y. Lvov, *ACS Sustainable Chem. Eng.*, 2017, **5**, 1775–1783.

15 Ş. Öncel, B. Kurtoğlu and B. Karaağaç, *J. Elastomers Plast.*, 2018, **51**, 440–456.

16 R. R. Espinosa, R. Inchingolo, S. M. Alencar, M. T. Rodriguez-Estrada and I. A. Castro, *Food Chem.*, 2015, **182**, 95–104.

17 M. S. Brewer, *Compr. Rev. Food Sci. Food Saf.*, 2011, **10**, 221–247.

18 E. Zerazion, R. Rosa, E. Ferrari, P. Veronesi, C. Leonelli, M. Saladini and A. M. Ferrari, *Green Chem.*, 2016, **18**, 1807–1818.

19 J. L. Koontz, J. E. Marcy, S. F. O'Keefe, S. E. Duncan, T. E. Long and R. D. Moffitt, *J. Appl. Polym. Sci.*, 2010, **117**, 2299–2309.

20 R. Guitard, J. F. Paul, V. Nardello-Rataj and J. M. Aubry, *Food Chem.*, 2016, **213**, 284–295.

21 B. Kirschweng, D. Tátraaljai, E. Földes and B. Pukánszky, *Polym. Degrad. Stab.*, 2017, **145**, 25–40.

22 S. Al-Malaika, H. Ashley and S. Issenhuth, *J. Polym. Sci., Part A: Polym. Chem.*, 1994, **32**, 3099–3113.

23 F. P. Byrne, B. Forier, G. Bossaert, C. Hoebers, T. J. Farmer and A. J. Hunt, *Green Chem.*, 2018, **20**, 4003–4011.

24 R. S. Borges, T. G. Barros, A. A. S. Veiga, A. S. Carneiro, C. A. L. Barros and A. B. F. da Silva, *Med. Chem. Res.*, 2015, **24**, 3453–3459.

25 K. Doudin, S. Al-Malaika, H. H. Sheena, V. Tverezovskiy and P. Fowler, *Polym. Degrad. Stab.*, 2016, **130**, 126–134.

26 M. Xin, Y. Ma, K. Xu and M. Chen, *J. Therm. Anal. Calorim.*, 2013, **114**, 1167–1175.

27 J. R. Perilla, B. C. Goh, C. K. Cassidy, B. Liu, R. C. Bernardi, T. Rudack, H. Yu, Z. Wu and K. Schulten, *Curr. Opin. Struct. Biol.*, 2015, **31**, 64–74.

28 Y. Luo, R. Wang, S. Zhao, Y. Chen, H. Su, L. Zhang, T. W. Chan and S. Wu, *RSC Adv.*, 2016, **6**, 58077–58087.

29 K. Luo, G. You, X. Zhao, L. Lu, W. Wang and S. Wu, *Mater. Des.*, 2019, **181**, 107944–107957.

30 S. Yu, Y. Wang, Y. Ma, L. Wang, J. Zhu and S. Liu, *Inorg. Chim. Acta*, 2017, **468**, 159–170.

31 K. Luo, W. Zheng, X. Zhao, X. Wang and S. Wu, *Mater. Des.*, 2018, **154**, 312–325.

32 B. Qiao, X. Zhao, D. Yue, L. Zhang and S. Wu, *J. Mater. Chem.*, 2012, **22**, 12339–12348.

33 K. Golzar, S. Amjad-Iranagh, M. Amani and H. Modarress, *J. Membr. Sci.*, 2014, **451**, 117–134.

34 Y. Zou, Y. Sun, Y. Zhang, J. He, Z. Tang, L. Zhu, Y. Luo and F. Liu, *Polym. Degrad. Stab.*, 2016, **133**, 201–210.

35 C. S. Abraham, S. Muthu, J. C. Prasana, S. J. Armakovic, S. Armakovic, B. F. Rizwana and A. S. Ben Geoffrey, *Comput. Biol. Chem.*, 2018, **77**, 131–145.

36 L. He, W. Li, D. Chen, J. Yuan, G. Lu and D. Zhou, *Appl. Surf. Sci.*, 2018, **440**, 331–340.

37 Y. Wang, G. Yang, W. Wang, S. Zhu, L. Guo, Z. Zhang and P. Li, *J. Mol. Liq.*, 2019, **277**, 261–268.

38 L. Wang, F. Yang, X. Zhao and Y. Li, *Food Chem.*, 2019, **275**, 339–345.

39 X. Chen, C. Yuan, C. K. Wong and G. Zhang, *J. Mol. Model.*, 2012, **18**, 2333–2341.

40 P. Bačová, L. G. D. Hawke, D. J. Read and A. J. Moreno, *Macromolecules*, 2013, **46**, 4633–4650.

41 C. Marteau, R. Guitard, C. Penverne, D. Favier, V. Nardello-Rataj and J. M. Aubry, *Food Chem.*, 2016, **196**, 418–427.

42 Y. Ren, Z. Y. Zhang, R. T. Lan, L. Xu, Y. Gao, B. Zhao, J. Z. Xu, R. M. Gul and Z. M. Li, *Mater. Sci. Eng., C*, 2019, **94**, 211–219.

43 J. Xue, Y. Niu, M. Gong, R. Shi, D. Chen, L. Zhang and Y. Lvov, *ACS Nano*, 2015, **9**, 1600–1612.

44 J. L. Koenig, *Spectroscopy of polymers*, Elsevier, 1999.

45 L. Huang, J. Ma, X. Wang, P. Zhang, L. Yu and S. Zhang, *Tribol. Int.*, 2018, **121**, 114–120.

46 Y. H. Lee, M. Cho, J.-D. Nam and Y. Lee, *Polym. Degrad. Stab.*, 2018, **148**, 50–55.

47 N. Sahiner, S. Sagbas, M. Sahiner, C. Silan, N. Aktas and M. Turk, *Int. J. Biol. Macromol.*, 2016, **82**, 150–159.